

Effects of Biosilicate[®] Scaffolds and Low-Level Laser Therapy on the Process of Bone Healing

Karina Nogueira Zambone Pinto, PhD,¹ Carla Roberta Tim, MS,² Murilo Camuri Crovace, MS,³
Mariza Akemi Matsumoto, PhD,⁴ Nivaldo Antonio Parizotto, PhD,¹
Edgar Dutra Zanotto, PhD,³ Oscar Peitl, PhD,³ and Ana Claudia Muniz Rennó, PhD⁵

Abstract

Objective: This study aimed to investigate the *in vivo* tissue performance of the association of Biosilicate[®] scaffolds and low-level laser therapy (LLLT) in a tibial bone defects model in rats. **Background data:** Many studies have been demonstrating the osteogenic potential of Biosilicate and LLLT. However, there is a need to investigate the effects of both treatments for bone consolidation. **Methods:** The animals were divided into control group (CG), Biosilicate scaffold group (BG), and Biosilicate scaffolds plus LLLT group (BLG). Animals were euthanized after 15, 30, and 45 days post-injury. **Results:** The histological analysis revealed that all the experimental groups showed inflammatory infiltrate and granulation tissue, at the area of the defect at day 15. After 30 days, CG still showed granulation tissue and bone ingrowth. Both Biosilicate groups presented newly formed bone and interconnected trabeculae. At 45 days, CG showed immature newly formed bone. A more mature newly formed bone was observed in BG and BLG. On day 15, BG demonstrated a statistically higher expression of cyclooxygenase (COX)-2 compared with CG and BLG. No statistically significant difference was observed in COX-2 immunoexpression among the groups at 30 and 45 days. Similar expression of bone morphogenetic protein (BMP)-9 was demonstrated for all experimental groups at 15 and 30 days. At 45 days, the BMP-9 immunoexpression was statistically upregulated in the BLG compared with the CG and BG. No statistically significant difference was observed in the receptor activator of nuclear factor kappa-B ligand (RANKL) immunoexpression among the groups in all periods evaluated. Biosilicate groups presented a decrease in biomechanical properties compared with CG at 30 and 45 days post-surgery. **Conclusions:** Our findings suggest that Biosilicate presented osteogenic activity, accelerating bone repair. However, laser therapy was not able to enhance the bioactive properties of the Biosilicate.

Introduction

BIOACTIVE GLASS HAS BEEN WIDELY USED AS A MATERIAL FOR bone substitution, mainly because of its unique ability to bond to living tissue, and its biocompatibility and osteoconductive properties.^{1,2} Its osteointegration is related to the formation of a silica gel layer, which acts as a template for calcium phosphate precipitation, which attracts fibronectin, macrophages, mesenchymal stem cells, and osteoprogenitor cells.^{2–5} The osteoprogenitor cells proliferate and differentiate in osteoblasts and the synthesis and deposition of the organic matrix starts. Thus, the organic matrix undergoes a gradual mineralization process guided by the osteoblastic cells.⁵

One of the most frequently studied bioactive glass is the 45S5 Bioglass[®], and it is known as one of the most bioactive and osteogenic materials.^{2,6} Despite its well-known stimulatory effects on osteogenesis, the use of monolithic 45S5 Bioglass for bone engineering applications has been limited, because of its relatively poor mechanical properties.^{2,6} Considering this important issue, our research group has designed specific nucleation and growth thermal treatments to obtain a novel fully crystallized bioactive glass-ceramic of the same quaternary P₂O₅-Na₂O-CaO-SiO₂ system, with some compositional modification (Biosilicate[®], patent application WO2004/074199).⁷ Biosilicate promoted enhanced bone-like matrix formation in comparison with its parent glass and with Bioglass 45S5 in an osteogenic cell culture

¹Department of Morphology, Federal University of São Carlos, São Carlos, São Paulo, Brazil.

²Department of Physiotherapy, Federal University of São Carlos, São Carlos, São Paulo, Brazil.

³Department of Materials Engineering, Federal University of São Carlos, São Carlos, São Paulo, Brazil.

⁴Department of Oral Maxillofacial Surgery, School of Dentistry, University of the Sacred Heart, Bauru, São Paulo, Brazil.

⁵Department of Bioscience, Federal University of São Paulo, Santos, Sao Paulo, Brazil.

system.⁸ Moreover, Biosilicate was efficient to induce bone formation and to improve the biomechanical properties of the bone callus in a tibial bone defect model.⁹

Similarly, low-level laser therapy (LLLT) has a positive effect on bone tissue metabolism and on fracture consolidation.^{10,11} When laser light is applied to living tissue, it is absorbed by chromophore photoreceptors located in the cells. Once absorbed, light can modulate cell biochemical reactions and stimulate mitochondrial respiration, with the production of molecular oxygen and adenosine triphosphate (ATP) synthesis.¹² *In vitro* studies using osteoblastic cells showed that LLLT is able to increase mitochondrial activity,¹³ osteoblast DNA and RNA synthesis, bone nodule formation,¹⁴ osteocalcin and osteopontin gene expression, and alkaline phosphatase (ALP) activity.¹² Also, LLLT has demonstrated the ability to accelerate the process of fracture repair in rabbits and rats, increasing the callus volume and bone mineral density.^{15,16}

Although the positive effects of Biosilicate and LLLT on bone cell proliferation and bone healing have already been demonstrated, the effects of the association of both therapies on bone consolidation have not been studied yet. In view of the aforementioned, it was hypothesized that the use of both treatments could enhance the bioactivity of the material, providing a bone graft with additional advantages for clinical use. Consequently, the present study aimed to evaluate the *in vivo* tissue response of the Biosilicate scaffolds and LLLT in a tibial bone defect model in rats.

Material and Methods

This study was conducted in accordance with the Guide for Care and Use of Laboratory Animals, and approved by the Animal Ethics Committee of the Federal University of São Carlos (002/2009). The animals were maintained under controlled temperature ($24 \pm 2^\circ\text{C}$), light-dark periods of 12 h. They were housed in plastic cages and had free access to water and standard food.

Male Wistar rats (12 weeks, weight ± 250 g, $n=90$) were randomly divided into three groups: control group (CG), Biosilicate scaffold group (BG), and Biosilicate scaffold irradiated with laser group (BLG). Each group was divided into three subgroups, euthanized by carbon dioxide asphyxia on days 15, 30, and 45 post-surgery. The tibiae were defleshed and removed for analysis.

Surgery

Bilateral noncritical size bone defects were surgically created at the upper third of the tibia (10 mm distal of the knee joint). Surgery was performed under sterile conditions and general anesthesia induced by intraperitoneal injection of ketamine/xylazine (80/10 mg/kg). The medial compartment of the tibia was exposed through a longitudinal incision on the shaved skin. A standardized 3.0 mm diameter bone defect was created by using a motorized drill under copious irrigation with saline solution. Immediately afterwards, a Biosilicate scaffold was implanted in the bone cavities, with the exception of the control animals. The cutaneous flap was replaced, sutured with resorbable polyglactin (Johnson & Johnson, St. Stevens-Woluwe, Belgium) and the skin was disinfected with povidone iodine. The health status of the rats was monitored daily.^{9,17}

Biosilicate scaffold

A fully crystallized bioactive glass-ceramic of the quaternary Na₂O-CaO-SiO₂-P₂O₅ system (Biosilicate, patent application WO2004/074199)⁷ was utilized. This compound has been described previously.¹⁸ Scaffolds were prepared through the addition of a polyethylene fibers into a cement based on powdered Biosilicate. The mixture was maintained under vigorous stirring during 30 min, until the formation of a homogeneous gel. Biosilicate powder (particle size $\sim 5\mu\text{m}$) was added to the gel in a proportion of 40% vol. and homogenized with a glass rod. Thus, 15% vol. of polyethylene fibers (Flinco) 3.2 mm long and 0.22 mm thick were added to the mixture, and again homogenized. The cement was poured in an alumina-zirconia-silica crucible and dried at room temperature for 72 h. Blocks of $\sim 50 \times 80 \times 16$ mm were obtained and through an odontologic trephine bur (WMA[®]), and scaffolds of 3.0 mm diameter and 1.5 mm thickness were obtained (mean pore diameters of 230 μm and total porosity of 44%).

LLLT

A low-energy Ga-Al-As (Teralaser, DMC[®] São Carlos-SP, Brazil), 830 nm, continuous wave laser, 0.028 cm² beam diameter, power 100 mW, power density 3.57 W/cm², fluence 120 J/cm², with a irradiation time of 34 sec (total energy 3.4 J), was used in this study. Laser irradiation was initiated immediately after the bone defect surgery and it was conducted each 48 h, in a total of 8, 15, and 23 sessions, depending upon the time of euthanasia (15, 30, and 45 days post-surgery, respectively). The irradiation was performed at one point, above the area of the injury, through the punctual contact technique.

Histopathological analysis

The right tibiae were removed and fixed in 10% buffer formalin (Merck, Darmstadt-Germany) for 48 h, decalcified in 4% ethylenediaminetetraacetic acid (EDTA) (Merck) and embedded in paraffin blocks. Five micrometer slices were obtained in a serially longitudinal sectioned pattern. Three sections of each specimen were stained with hematoxylin and eosin (H & E, Merck) and examined using light microscopy (Olympus, Optical Co. Ltd, Tokyo-Japan, magnification of 40 \times). Any changes in the bone defect were qualitatively analyzed, such as presence of woven bone, medullar tissue, inflammatory process, and granulation tissue.¹⁷ This analysis was performed by an experienced pathologist in a blinded manner.

Immunohistochemistry

Paraffin was removed with xylene from serial sections of 5 μm , and the sections were rehydrated in graded ethanol, and then pretreated in a microwave with 0.01 M citric acid buffer, pH 6, for three cycles of 5 min each at 850 W for antigen retrieval. Three sections of each specimen were incubated with polyclonal primary antibodies anti-cyclooxygenase (COX)-2, anti-bone morphogenetic protein (BMP)-9 and anti-receptor activator of nuclear factor kappa-B ligand (RANKL), all at a concentration of 1:200 (Santa Cruz Biotechnology, CA). The sections were then incubated with

biotin conjugated secondary antibody anti-rabbit IgG (Vector Laboratories, Burlingame, CA) at a concentration of 1:200 in phosphate-buffered saline (PBS) for 1 h. The sections were washed twice with PBS followed by the application of pre-formed avidin biotin complex conjugated to peroxidase (Vector Laboratories) for 45 min. The bound complexes were visualized by the application of a 0.05% solution of 3-3'-diaminobenzidine solution and counterstained with Harris hematoxylin. For control studies of the antibodies, the serial sections were treated with rabbit immunoglobulin G (IgG) (Vector Laboratories) at a concentration of 1:200 in place of the primary antibody. Additionally, internal positive controls were performed with each staining bath.

COX-2, BMP-9, and RANKL immunoevaluations were evaluated both qualitatively (presence of the immunomarkers) and semi-quantitatively in five predetermined fields using a light microscope (Leica Microsystems AG, Wetzlar, Germany). According to previous studies, the quantity of positive cells per field was described by a scoring scale from 1 to 4 (1=absent, 2=weak, 3=moderate, and 4=intense).^{19,20} The

analysis was performed by two observers (C.T. and K.N.Z.), in a blinded manner.

Biomechanical analysis

The maximum load at failure (kN) was determined by a three point bending test with a 1 kN load (Instron® Universal Testing Machine, USA, 4444 model). Tibiae were placed on a 3.8 cm metal device, which provided a 1.8 cm distance between the two supports. The load cell was perpendicularly positioned in the anterior-posterior direction at the exact site of the bone defect. A 5 N preload was applied in order to avoid specimen sliding. Finally, the bending force was applied at a constant deformation rate of 0.5 cm/min until fracture occurred.

Statistical analysis

Data were expressed as mean values and standard deviations (SD). Comparisons among the groups were made using one way analysis of variance (ANOVA),

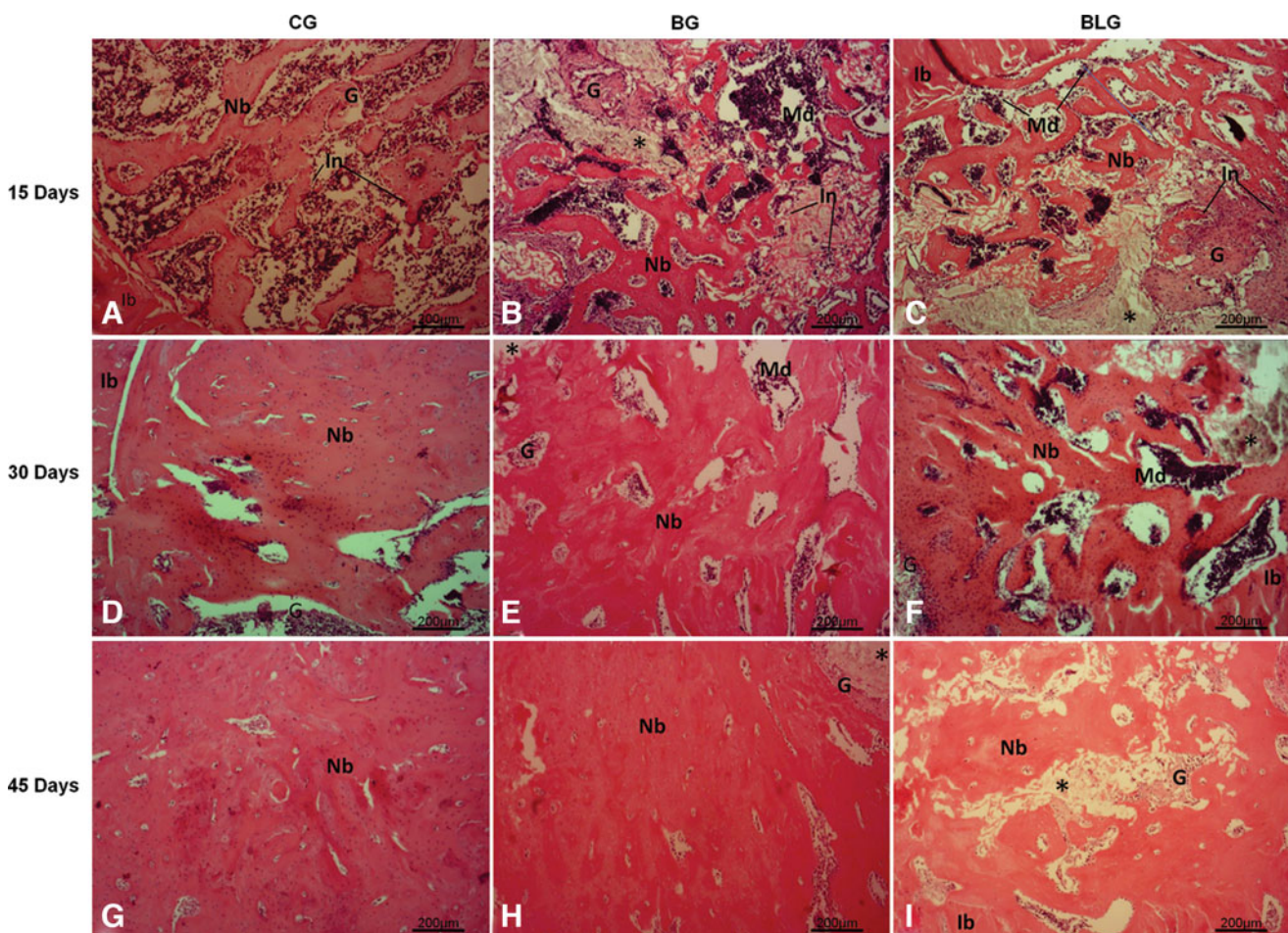


FIG. 1. Representative histological sections of experimental groups. Intact bone (Ib), newly formed bone (Nb), granulation tissue (G), inflammatory infiltrate (In), medullar tissue (Md). Biomaterial particles (asterisk). (A) Control group 15 days. (B) Biosilicate® group 15 days. (C) Biosilicate+low-level laser therapy (LLLT) group 15 days. (D) Control group 30 days. (E) Biosilicate group 30 days. (F) Biosilicate+LLLT group 30 days. (G) Control group 45 days. (H) Biosilicate group 45 days. (I) Biosilicate+LLLT group 45 days (hematoxylin and eosin [H.E.] stain).

complemented by Duncan's test post-test analysis, considering $p \leq 0.05$.

Results

At the moment of the retrieval of the specimens, a satisfactory healing process of the injured bone was noted, and no infection in the surgical site was observed (data not shown).

Histopathological analysis

In the CG, the edges of the bone defect were clearly visible after 15 days. Also, the defects were filled with inflammatory infiltrate and granulation tissue, with the presence of woven bone with no interconnected trabeculae (Fig. 1A). In BG and BLG, similar histological findings were observed, with inflammatory infiltrate, granulation tissue, and newly formed bone surrounding the Biosilicate particles, which were partially degraded in both groups (Fig. 1B and C).

On day 30, the edges of the injury were still evident in the CG. Granulation tissue filled most of the area of the defect, but in some regions, bone ingrowth was observed (Fig. 1D). In the BG, the particles of the biomaterial still could be

noticed. Newly formed bone filled the spaces occupied by the degraded biomaterial. Furthermore, most of the remaining particles were surrounded by newly formed bone, with interconnected trabeculae. Sporadically, granulation tissue was found around the particles (Fig. 1E). Regarding the BLG, newly formed bone and granulation tissue were observed surrounding the particles. Moreover, newly formed bone was observed but it seems to be more disorganized in comparison to the BG (Fig. 1F).

After 45 days, newly formed bone had grown into the area of the defects in the CG. Most of the newly formed bone presented an organized tissue structure, with interconnected trabeculae (Fig. 1G). In the BG specimens, some Biosilicate particles still could be seen. The defect was filled with organized newly formed bone (Fig. 1H). In the BLG, only a few particles of Biosilicate were detected. The defect was filled with newly formed bone tissue. However, its structure was less organized than that of the BG. In some cases, granulation tissue still could be observed (Fig. 1I).

Immunohistochemistry

COX-2. After 15 days, the CG showed the expression of the COX-2 mainly at the medullar tissue (Fig. 2A). In the BG

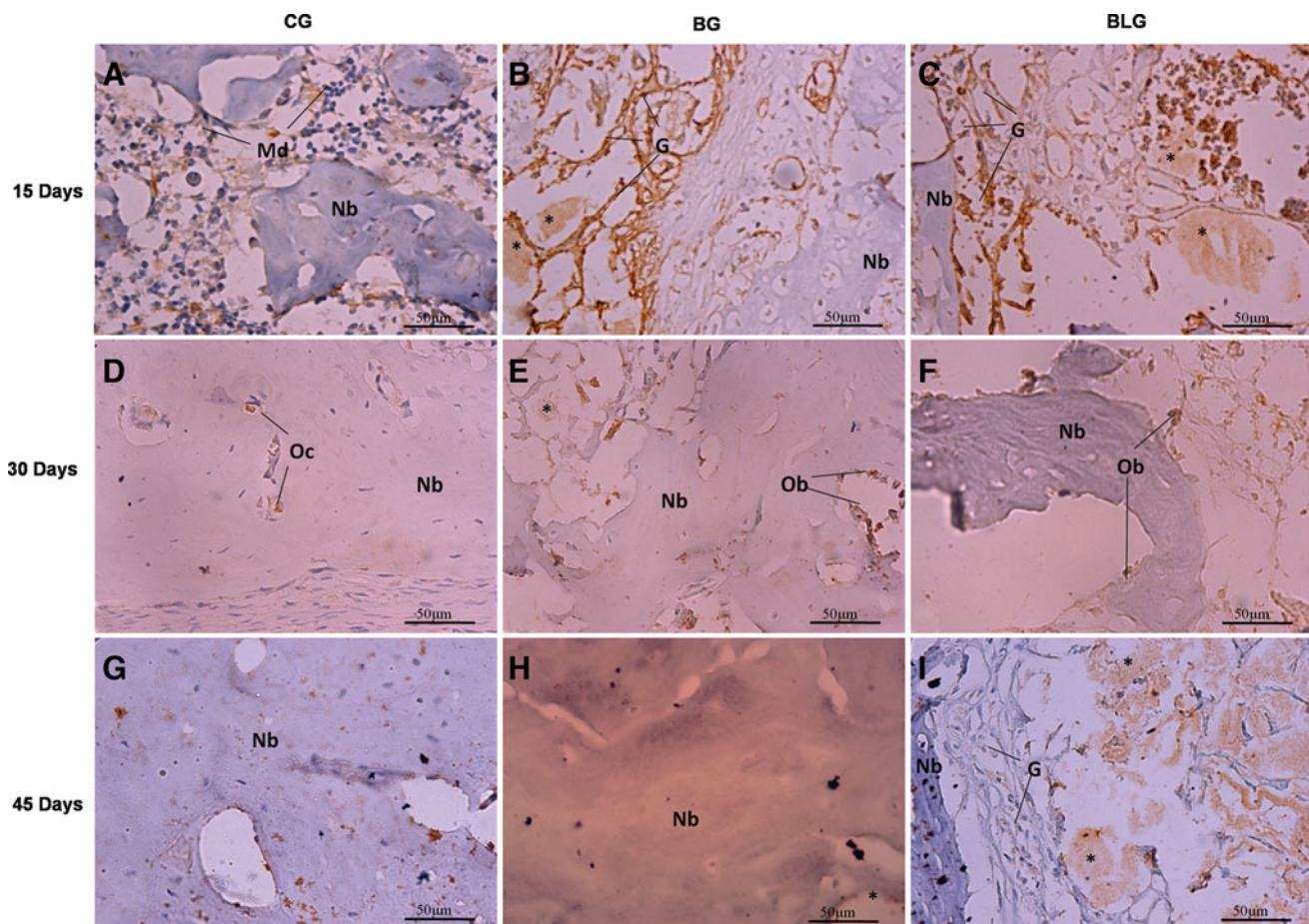


FIG. 2. Representative sections of cyclooxygenase (COX)-2 immunohistochemistry. Immunoexpression in medullar tissue (Md), granulation tissue (G), osteocytes (Oc), osteoblasts (Ob), and newly formed bone (Nb). Biomaterial particles (asterisk). (A) Control group 15 days. (B) Biosilicate® group 15 days. (C) Biosilicate+ low-level laser therapy (LLLT) group 15 days. (D) Control group 30 days. (E) Biosilicate group 30 days. (F) Biosilicate+LLLT group 30 days. (G) Control group 45 days. (H) Biosilicate group 45 days. (I) Biosilicate+LLLT group 45 days.

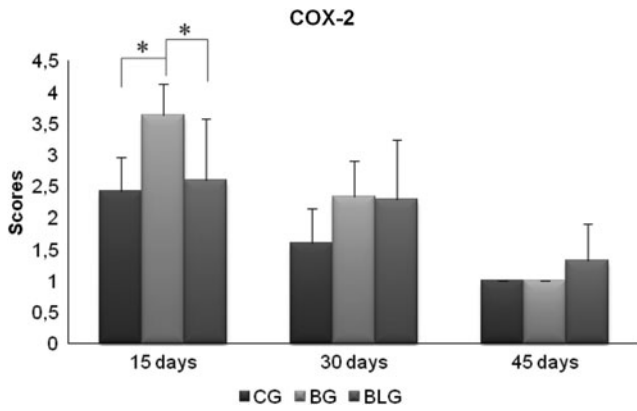


FIG. 3. Mean and SD scores for immunostaining of cyclooxygenase (COX)-2. CG, control group; BG, Biosilicate® scaffold; BLG, Biosilicate+low-level laser therapy (LLLT). Significant differences of $p < 0.05$ are represented by a single asterisk (*).

and BLG, the immunorexpression of COX-2 was evident in cells of the granulation tissue around the biomaterial particles (Fig. 2B and C). However, the BG demonstrated a statistically higher expression of COX-2 than did the CG ($p = 0.01439$) and BLG ($p = 0.02740$) (Fig. 3).

On day 30, COX-2 expression could be observed in the osteoblasts and osteocytes of CG (Fig. 2D). Figures 2E and F show that COX-2 expression was observed in the osteoblasts of the BG and BLG. In the last period evaluated, immunorexpression of COX-2 was not observed for the CG and BG (Figs. 2G and H). In the BLG, COX-2 was immunorexpressed in the granulation tissue surrounding the particles (Fig. 2I). Nevertheless, no difference in COX-2 immunorexpression was found among the groups on days 30 and 45 (Fig. 3).

BMP-9. On the 15th day, the CG showed immunorexpression of BMP-9 mainly at the medullar tissue (Fig. 4A). The immunorexpression of BMP-9 was detected for the BG and BLG in cells of the granulation tissue (Fig. 4B and C). After 30 days, immunorexpression of BMP-9 was detected for all groups in the granulation tissue and in osteoblasts (Fig. 4D–F). On days 15 and 30, no statistically significant differences in the BMP-9 immunolabeling among the groups were observed (Fig. 5).

The CG did not show expression of BMP-9 on the 45th day (Fig. 4G). In the BG and BLG, BMP-9 expression was detected in osteoblasts and in the granulation tissue surrounding the biomaterial particles (Fig. 4H and I). On day 45, the BLG presented a statistically higher expression of BMP-9 than did the CG ($p = 0.00001$) and BG ($p = 0.00002$) (Fig. 5).

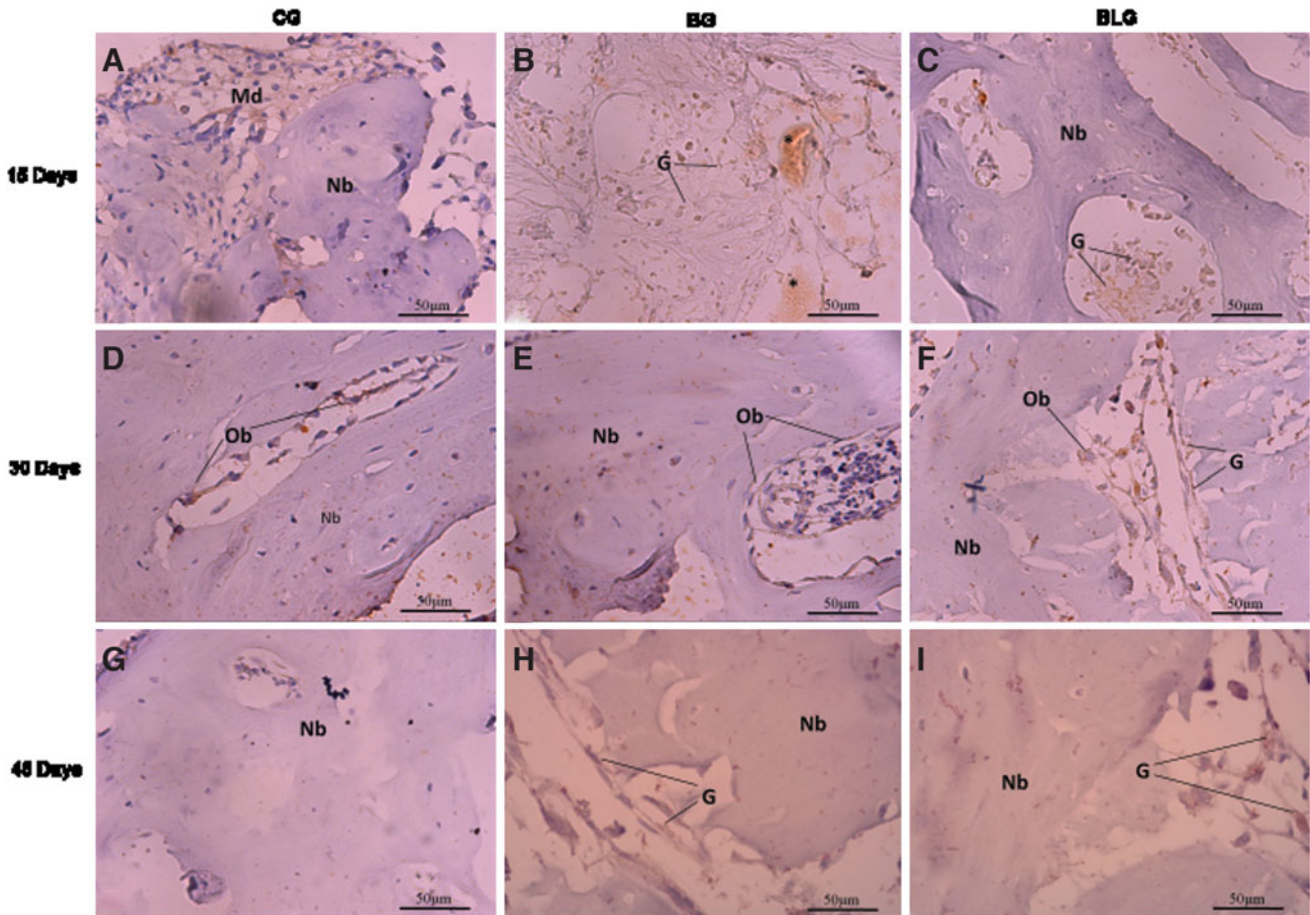


FIG. 4. Representative sections of bone morphogenetic protein (BMP)-9 immunohistochemistry. Immunorexpression in medullar tissue (Md), granulation tissue (G), osteoblasts (Ob), and newly formed bone (Nb). Biomaterial particles (*asterisk*). (A) Control group 15 days. (B) Biosilicate® group 15 days. (C) Biosilicate+low-level laser therapy (LLLT) group 15 days. (D) Control group 30 days. (E) Biosilicate group 30 days. (F) Biosilicate+LLLT group 30 days. (G) Control group 45 days. (H) Biosilicate group 45 days. (I) Biosilicate+LLLT group 45 days.

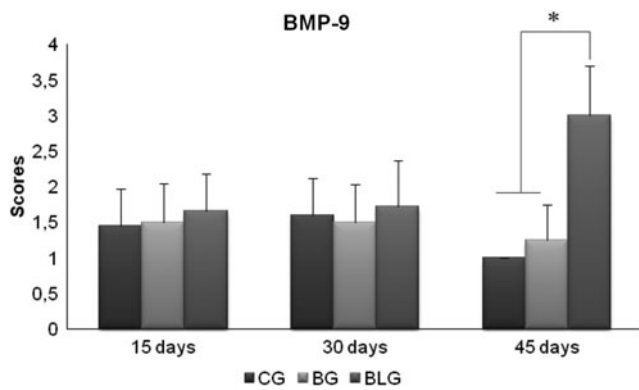


FIG. 5. Mean and SD scores for immunostaining of bone morphogenetic protein (BMP)-9. CG, control group; BG, Biosilicate® scaffold group; BLG, Biosilicate+low-level laser therapy (LLLT) group. Significant differences of $p < 0.05$ are represented by a single asterisk (*).

RANKL. On day 15, RANKL expression was evident in medullar tissue in the CG, whereas the immunolabeling of this protein was present in the granulation tissue, especially around the Biosilicate particles, in the BG and BLG (Fig. 6A–C). After 30 days, in all groups, the immunoexpression of

RANKL was present at the cells of granulation tissue, surrounding biomaterial particles in BG and BLG (Fig. 6D–F). On day 45, the expression of the RANKL was observed in osteocytes of the CG and BG, and at the cells of granulation tissue in the BLG (Fig. 6G–I).

No statistically significant difference was observed in the RANKL immunoexpression among the groups in all evaluated periods (Fig. 7).

Biomechanical analysis

After 15 days, no statistically significant differences in the maximum load among the groups were observed. On day 30, the BG ($p = 0.01632$) and BLG ($p = 0.00011$) showed statistically lower values than did the CG. Similarly, after 45 days, the BG ($p = 0.00049$) and BLG ($p = 0.00205$) presented statistically lower values than did the CG (Fig. 8).

Discussion

In this study, the *in vivo* response to the association of Biosilicate scaffolds and LLLT was evaluated in a rat tibial bone defect model. It was hypothesized that laser therapy could enhance the bioactive properties of the Biosilicate scaffolds, which would culminate in the increase in bone formation.

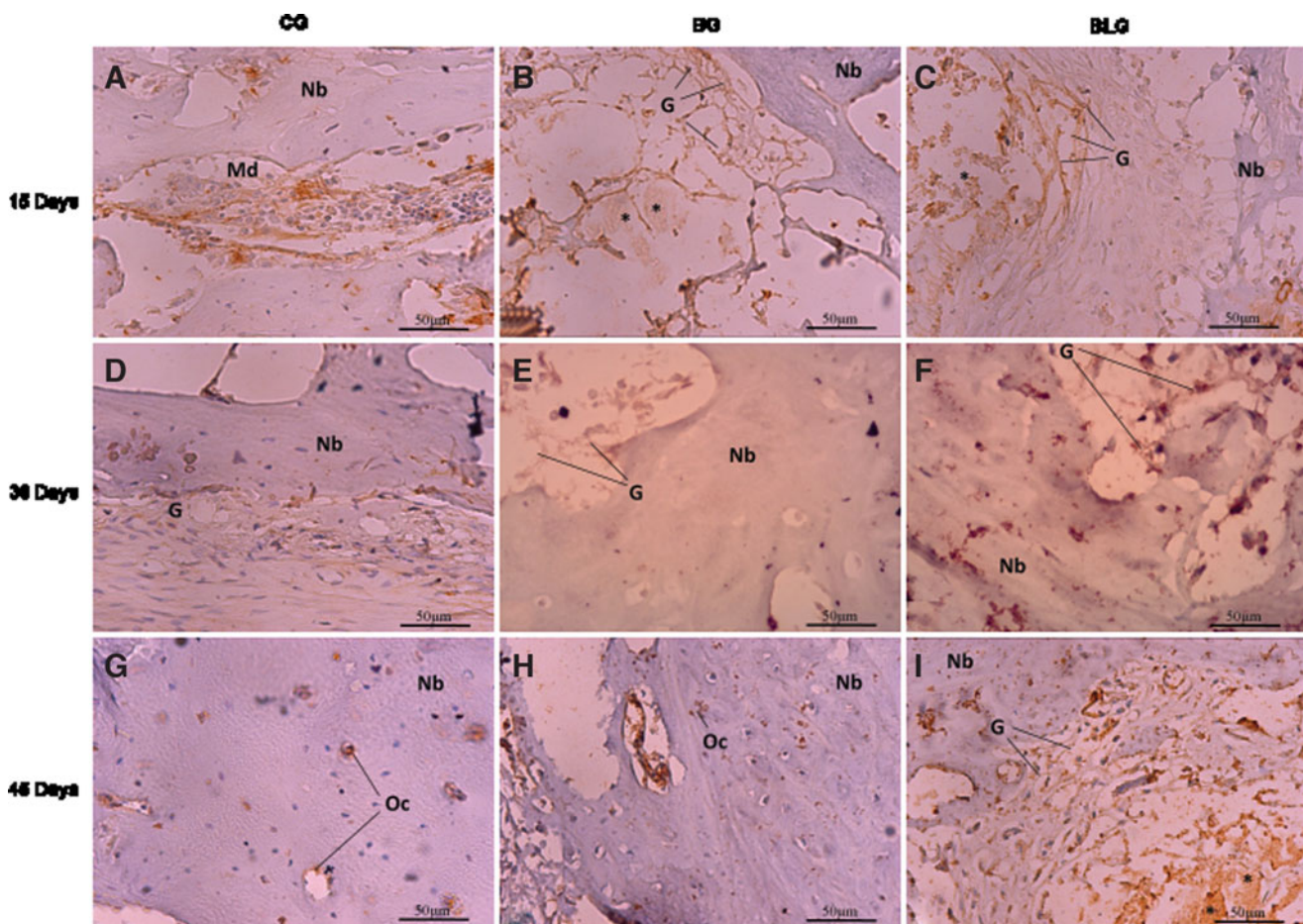


FIG. 6. Representative sections of receptor activator of nuclear factor kappa-B ligand (RANKL) immunohistochemistry. Immunoexpression in medullar tissue (Md), granulation tissue (G), osteocytes (Oc), and newly formed bone (Nb). Biomaterial particles (asterisk). (A) Control group 15 days. (B) Biosilicate® group 15 days. (C) Biosilicate+low-level laser therapy (LLLT) group 15 days. (D) Control group 30 days. (E) Biosilicate group 30 days. (F) Biosilicate+LLLT group 30 days. (G) Control group 45 days. (H) Biosilicate group 45 days. (I) Biosilicate+LLLT group 45 days.

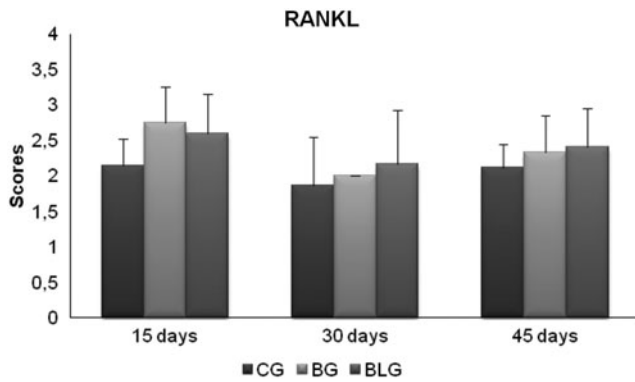


FIG. 7. Mean and SD scores for immunostaining of receptor activator of nuclear factor kappa-B ligand (RANKL). CG, control group; BG, Biosilicate® scaffold group; BLG, Biosilicate + low-level laser therapy (LLLT) group.

Bioactive glasses have been used as bone graft substitutes because of their ability to bond and to integrate with living bone by forming a biologically active bone-like apatite layer on their surfaces.¹⁻³ In an *in vivo* study, Matsumoto et al.²⁰ showed that Biosilicate stimulated bone formation during the process of bone defect healing. These findings are in line with the results of the current study, which demonstrated that the BG presented organized newly formed bone around the particles of biomaterial.

Moreover, laser therapy is a promising noninvasive method for stimulating osteogenesis and accelerating bone healing.^{21,22} It was expected that the association of the osteogenic potential of bioactive glass and LLLT would culminate in an earlier resolution of the inflammatory process and a higher recruitment of bone cells. However, the histological findings showed that BLG animals presented less organized newly formed bone than did BG animals, demonstrating that LLLT was not effective in producing any extra stimulus to tissue for bone healing improvement.

The effects of Biosilicate and LLLT *in vitro* and *in vivo* experiments have been investigated, and the results are controversial.^{9,17,23-25} In an *in vivo* study, Oliveira et al.¹⁷ associated laser therapy (60 or 120 J/cm²) with particulate

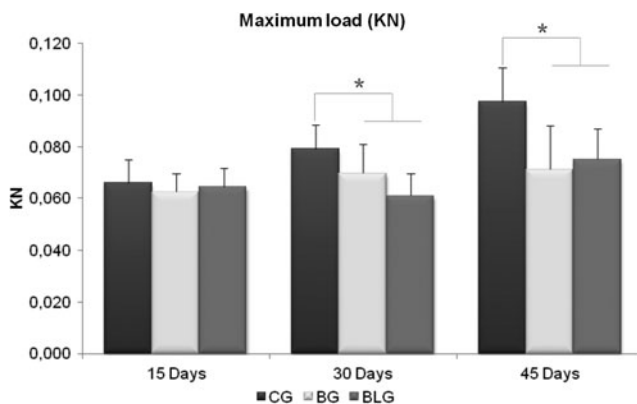


FIG. 8. Means and SD of maximum load. CG, control group; BG, Biosilicate® scaffold group. BLG, Biosilicate + low-level laser therapy (LLLT). Significant differences of $p < 0.05$ are represented by a single asterisk (*).

Biosilicate on bone defect healing treatment on healthy rat models, and showed that laser therapy was not able to improve the effects of particulate Biosilicate. On the other hand, Fangel et al.²⁵ and Bossini et al.²³ showed that particulate Biosilicate (180–212 μm) associated with LLLT (830 nm) was capable of inducing bone formation on bone defects of osteoporotic rats. In this study, the lack of beneficial effects produced by LLLT in Biosilicate-treated animals may be related to the laser fluence and energy output used during the treatment in healthy rats. The amount of laser energy applied to the tissue plays an important role in the biological response, and the existence of a dose-response curve is well known.²³⁻²⁵ Therefore, the hypothesis that the laser parameters used in this study were not sufficient to offer an extra stimulus for accelerating bone healing can be raised.

Also, COX-2 expression was upregulated in the BG on the 15th day. COX-2 is the rate-limiting enzyme in the conversion of arachidonic acid to prostaglandins, which have effects on the proliferation and differentiation of osteoblasts, and regulate the differentiation and function of osteoclasts.^{16,26} It may be suggested that the earlier appearance of COX-2 in the BG was responsible for the earlier recruitment of inflammatory cells observed in the histological analysis, resulting in a more organized newly formed bone tissue. These findings corroborate those of Bossini et al.²³ in osteoporotic rats.

BMPs exhibit stimulatory properties to differentiation of mesenchymal cells into osteogenic/chondrogenic lineage, and increase expression of alkaline phosphatase and osteocalcin.^{27,28} The immunohistochemical analysis revealed that the BLG showed a late peak of BMP-9 expression 45 days after surgery, in the granulation tissue still observed surrounding the biomaterial particles, corroborating to the delay in the bone repair presented by this group.

The RANKL is a key factor for osteoclast differentiation and activation.^{29,30} It has been demonstrated that cellular expression of RANKL in murine callus tissue is tightly coupled during fracture healing, and is involved in the regulation of both endochondral resorption and bone remodeling.³¹ The immunohistochemical analysis demonstrated a slightly higher immunolabeling of the RANKL around Biosilicate particles, irradiated with laser or not, on the 15th day. These findings suggest a higher amount of macrophages/osteoclasts on the surface of the material and an accelerated bone turnover, which could culminate in a faster healing.

In the biomechanical analysis, the BG and BLG showed statistically lower values of the maximum load than did the CG after 30 and 45 days. These results seem to be in accordance with a previous study in which particulate Biosilicate (180–212 μm) and laser (Ga-Al-As, 830 nm) were used to treat bone defects in healthy rats, and resulted in decreased mechanical properties.⁸ Conversely, Bossini et al.²³ observed an increase in the biomechanical properties of bone defects of osteopenic female rats filled with biomaterial after laser irradiation. Bone mass and the quality and arrangement of bone microstructural elements influence its mechanical properties.¹¹ Therefore, the lack of the improved load-bearing capacity and stiffness showed by the biomaterial groups probably mirrors the difference in the amount and/or spatial distribution of newly formed bone into the defect site among the groups.

Summarizing, the incorporation of Biosilicate scaffolds accelerates bone healing. In addition, laser therapy did

not produce any extra effect in bone metabolism in the Biosilicate-treated animals.

Conclusion

The Biosilicate scaffold exerts osteogenic activity during bone repair, evidenced by the activation of immunomarkers related to the tissue repair such as COX-2, BMP-9, and RANKL. However, LLLT was not able to enhance the bioactive properties of the Biosilicate scaffolds. Moreover, Biosilicate scaffolds, either associated with laser irradiation or not, were not effective in improving the mechanical properties of the bone callus. These data highlight the huge potential of the Biosilicate in bone regeneration applications. Further long-term studies should be developed in order to provide additional information concerning the late stages of bone matrix synthesis induced by Biosilicate and laser therapy used with different parameters.

Acknowledgments

We thank the Brazilian funding agencies Fundacao de Amparo a Pesquisa do estado de São Paulo (FAPESP) and Conselho nacional de desenvolvimento de pessoal de nivel superior (CNPQ) for the financial support of this research.

Author Disclosure Statement

No competing financial interests exist.

References

- Hollinger, J.O., Onikepe, A.O., MacKrell, J., Einhorn, T., Bradica, G., Lynch, S., and Hart, C.E. (2008). Accelerated fracture healing in the geriatric, osteoporotic rat with recombinant human platelet-derived growth factor-BB and an injectable beta-tricalcium phosphate/collagen matrix. *J. Orthop. Res.* 26, 83–90.
- Hench, L.L. (2006). The story of bioglass. *J. Mater. Sci. Med.* 17, 967–978.
- Peitl, O., Zanotto, E.D., Serbena, F.C., and Hench, L.L. (2012). Compositional and microstructural design of highly bioactive P2O5-Na2O-CaO-SiO2 glass-ceramics. *Acta Biomater.* 8, 321–332.
- Vogel, M., Voigt, C., Knabe, C., Radlanski, R.J., Gross, U.M., and Müller-Mai, C.M. (2004). Development of multinuclear giant cells during the degradation of Bioglass® particles in rabbits. *J. Biomed. Mater. Res. A.* 70, 370–379.
- Lu, H.H., Tang, A., Oh, S.C., Spalazzi, J.P., and Dionisio, K. (2005). Compositional effects on the formation of a calcium phosphate layer and the response of osteoblast-like cells on polymer-bioactive glass composites. *Biomaterials* 26, 6323–6334.
- Hench, L.L., and Wilson, J. (1984). Surface-active biomaterials. *Science* 226, 630–666.
- Fundação Universidade Federal de São Carlos, Universidade de São Paulo. Zanotto, E.D., et al. (2004). Process and compositions for preparing particulate, bioactive or resorbable biosilicates for use in the treatment of oral ailments. *Int. C. C03C10/00*, February 20, 2004, WO2004/074199.
- Moura, J., Teixeira, L.N., Ravagnani, C., Peitl Filho, O., Zanotto, E.D., Beloti, M.M., Panzeri, H., Rosa, A.L., and Oliveira, P.T. (2007). *In vitro* osteogenesis on a highly bioactive glass-ceramic (Biosilicate®). *J. Biomed. Mater. Res. A.* 82, 545–557.
- Granito, R.N., Rennó, A.C., Ravagnani, C., Bossini, P.S., Mochiuti, D., Jorgetti, V., Driusso, P., Peitl, O., Zanotto, E.D., Parizotto, N.A., and Oishi, J. (2011). *In vivo* biological performance of a novel highly bioactive glass-ceramic (Biosilicate®): a biomechanical and histomorphometric study in rat tibial defects. *J. Biomed. Mater. Res. B Appl. Biomater.* 97, 139–147.
- Luger, E.J., Rochkind, S., Wollman, Y., Kogan, G., and Dekel, S. (1998). Effect of low-power laser irradiation on the mechanical properties of bone fracture healing in rats. *Lasers Surg. Med.* 22, 97–102.
- Ozawa, Y., Shimizu, N., and Kariya, G. (1998). Low-energy laser irradiation stimulates bone nodule formation at early stages of cell culture in rat calvarial cells. *Bone* 22, 347–354.
- Yaiota, H., Orimo, H., Shirai, Y., and Shimada, T. (2000). Expression of bone morphogenetic proteins and rat distal-less homolog genes following rat femoral fracture. *J. Bone Miner. Metab.* 18, 63–70.
- Olivera, M.I., Martínez, M.P., Conti, M.I., Bozzini, C., Bozzini, C.E., and Alippi, R.M. (2008). Permanent reduction of mandibular size and bone stiffness induced in post-weaning rats by cyclophosphamide. *Arch. Oral Biol.* 54, 6–11.
- Stein, A., Benayahu, D., Maltz, L., and Oron, U. (2005). Low-level laser irradiation promotes proliferation and differentiation of human osteoblasts *in vitro*. *Photomed. Laser Surg.* 23, 61–166.
- Liu, X., Lyon, R., Meier, H.T., Thometz, J., and Haworth, S.T. (2007). Effect of lower-level laser therapy on rabbit tibial fracture. *Photomed. Laser Surg.* 25, 487–494.
- Matsumoto, M.A., Ferino, F.V., Monteleone, G.F., and Ribeiro, D.A. (2009). Low level laser therapy modulates cyclooxygenase-2 expression during bone repair in rats. *Lasers Med. Sci.* 24, 196–201.
- Oliveira, P., Ribeiro, D.A., Pipi, E.F., Driusso, P., Parizotto, N.A., and Rennó, A.C. (2010). Low-level laser therapy does not modulate the outcomes of a highly bioactive glassceramic (Biosilicate®) on bone consolidation in rats. *J. Mater. Sci. Mater. Med.* 21, 1379–1384.
- Hench, L.L. (2003). Glass and genes: The 2001 W. E. S. Turner Memorial Lecture. *Glass Technology* 44, 1–10.
- Pedrosa, W.F., Jr., Okamoto, R., Faria, P.E.P., Arnez, M.F.M., Xavier, S.P., and Salata, L.A. (2009). Immunohistochemical, tomographic and histological study on onlay bone grafts remodeling. Part II: calvarial bone. *Clin. Oral Implants Res.* 20, 1254–1264.
- Matsumoto, M.A., Caviquioli, G., Bigueti, C.C., Holgado, L.A., Saraiva, P.P., Rennó, A.C.M., and Kawakam, R.Y. (2012). A novel bioactive vitroceraamic presents similar biological responses as autogenous bone grafts. *J. Mater. Sci. Mater. Med.* 23, 1447–1456.
- Nissan, J., Assif, D., Gross, M.D., Yaffe, A., and Binderman, I. (2006). Effect of low intensity laser irradiation on surgically created bony defects in rats. *J. Oral Rehabil.* 3, 619–924.
- Pretel, H., Lizarelli, R.F.Z., and Ramalho, L.T.O. (2007). Effect of low-level laser therapy on bone repair: histological study in rats. *Lasers Surg. Med.* 39, 788–796.
- Bossini, P.S., Rennó, A.C.M., Ribeiro, D.A., Fangel, R., Peitl, O., Zanotto, E.D., and Parizotto, N.A. (2011). Biosilicate® and low-level laser therapy improve bone repair in osteoporotic rats. *J. Tissue Eng. Regen. Med.* 5, 229–237.
- Rennó, A.C.M., McDonnell, P.A., and Laakso, L. (2010). Effect of 830nm laser phototherapy on osteoblasts grown *in vitro* on Biosilicate® scaffolds. *Photomed. Laser Surg.* 28, 131–133.
- Fangel, R., Bossini, P.S., Rennó, A.C., Ribeiro, D.A., Wang, C.C., Toma, R.L., Okino, K., Driusso, P., Parizotto, N.A., and

- Oishi, J. (2011). Low-level laser therapy, at 60J/cm² associated with a Biosilicate® increase in bone deposition and indentation biomechanical properties of callus in osteopenic rats. *J. Biomed. Opt.* 16, 078001.
26. Zhang, X., Schwarz, E.M., Young, D.A., Puzas, E., Rosier, R.N., and O'Keefe, R.J. (2002). Cyclo-oxygenase-2 regulates mesenchymal cell differentiation into the osteoblast lineage and is critically involved in bone repair. *J. Clin. Invest.* 109, 1405–1415.
27. Proff, P., and Römer, P. (2009). The molecular mechanism behind bone remodelling: a review. *Clin. Oral Investig.* 13, 355–362.
28. Cheng, H., Jiang, W., Phillips, F.M., Haydon, R.C., Peng, Y., Zhou, L., Luu, H.H., An, N., Breyer, B., Vanichakarn, P., Szatkowski, J.P., Park, J.Y., and He, T.C. (2003). Osteogenic Activity of the fourteen types of human bone morphogenetic proteins (BMPs). *J. Bone Joint Surg. Am.* 85, 1544–1552.
29. Kearns, A.E., Khosla, S., and Kostenuik, P.J. (2008). Receptor activator of nuclear factor κ b ligand and osteoprotegerin regulation of bone remodeling in health and disease. *Endocr. Rev.* 29, 155–192.
30. Anandarajah, A.P. (2009). Role of RANKL in bone diseases. *Trends Endocrinol. Metab.* 20, 88–94.
31. Kon, T., Cho, T.J., Aizawa, T., Yamazaki, M., Nooh, N., Graves, D., Gerstenfeld, L.C., and Einhorn, T.A. (2001). Expression of osteoprotegerin, receptor activator of NF- κ B ligand (osteoprotegerin ligand) and related proinflammatory cytokines during fracture healing. *J. Bone Miner. Res.* 16, 1004–1014.

Address correspondence to:

Ana Claudia Rennó

Department of Bioscience

Federal University of Sao Paulo, Santos

Av. Ana Costa, 95

Santos

Brazil

E-mail: a.renno@unifesp.br